ELSEVIER

AppliedEnergy

# A 1000 MW$_{th}$ boiler for chemical-looping combustion of solid fuels – Discussion of design and costs

CrossMark

Anders Lyngfelt *, Bo Leckner

Chalmers University of Technology, 412 96 Göteborg, Sweden

## HIGHLIGHTS

- Chemical-Looping Combustion (CLC) is a novel combustion technology for $CO_2$ capture.
- CLC avoids large costs and energy penalties of gas separation for $CO_2$ capture.
- A scale-up of CLC technology for solid fuels to 1000 MW$_{th}$ is investigated.
- CLC technology is similar to CFB technology.
- Estimated cost of CLC with capture relative to CFB without capture is 20 €/tonne $CO_2$.

## ARTICLE INFO

## ABSTRACT

More than 2000 h of solid-fuel CLC operation in a number of smaller pilot units clearly indicate that the concept works. A scale-up of the technology to 1000 MW$_{th}$ is investigated in terms of mass and heat balances, flows, solids inventories, boiler dimensions and the major differences between a full-scale Circulating Fluidized-Bed (CFB) boiler and a Chemical-Looping Combustion CFB (CLC–CFB). Furthermore, the additional cost of CLC–CFB relative to CFB technology is analysed and found to be 20 €/tonne $CO_2$. The largest cost is made up of compression of $CO_2$, which is common to all capture technologies. Although the need for oxygen to manage incomplete conversion is estimated to be only a tenth of that of oxy-fuel combustion, oxygen production is nonetheless the second largest cost. Other significant costs include oxygen-carrier material, increased boiler cost and steam for fluidization of the fuel reactor.

## 1. Introduction

Chemical-looping combustion (CLC) has emerged as an attractive option for carbon dioxide capture because $CO_2$ is inherently separated from the other flue-gas components. Ideally, no gas separation equipment is needed and no energy is expended for gas separation. The CLC system is composed of two interconnected fluidized bed reactors, an air and a fuel reactor [1]. Oxygen carriers in the form of metal oxide particles transfer oxygen between the two reactors, Fig. 1.

CLC research has mainly been focusing on gaseous fuels but in the past few years, important work has been dedicated to adapting the process to solid fuels. A number of reviews are available for greater detail [2–5]. Lewis et al. [6] were the first to study solid fuels for CLC, using copper and iron oxides. Fifty years later, a number of new laboratory studies emerged employing the same oxides,

as well as manganese and nickel, involving testing in both fixed beds [7,8] and laboratory fluidized beds [9,10]. The first operation using solid fuels in a 10 kW unit was realized in 2006 [11] and today, a number of published articles address CLC pilot operation using solid fuel, e.g. [12–21].

It is the purpose of the present paper to discuss the design of a CLC boiler for solid fuel in view of the similarities to the well-known and commercially viable circulating fluidized-bed (CFB) technology, and furthermore, to identify the technology differences as well as the cost impact of those differences. Although techno-economic studies of the process have been performed in EU projects like ENCAP and ECLAIR, little detail about the designs and cost estimations of solid-fuel CLC boilers has been published.

### 1.1. Solid-fuel chemical-looping combustion

The direct use of solid fuels in CLC could employ the CFB concept outlined in Fig. 2, originally proposed for gaseous fuels, by adapting the fuel-reactor system to solid fuels. In Fig. 2 a

---

* Corresponding author.
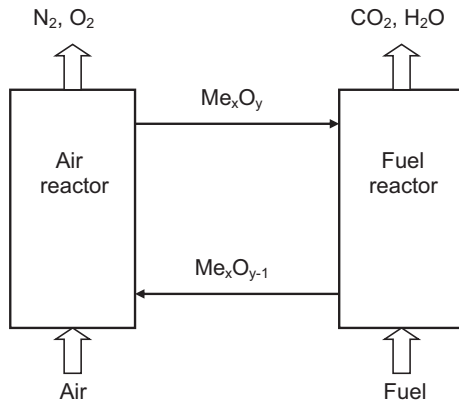   E-mail address: Anders.Lyngfelt@chalmers.se (A. Lyngfelt).

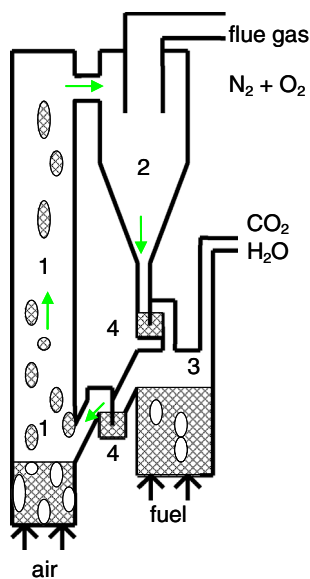Fig. 1. CLC principle. $Me_xO_y$ is the metal oxide circulated.



Fig. 2. CFB reactor system for gas, (1) air reactor, (2) cyclone, (3) fuel reactor (4) loop seals.



Fig. 3. Solid fuel reactions in CLC.



Fig. 4. Inadequate performance of the fuel reactor.

non-circulating fuel reactor is depicted, but for a commercial-scale unit a circulating fuel reactor would be preferred. With solid fuels, the reaction between the char remaining after the release of the volatiles and the oxygen carrier is not direct but involves an intermediate gasification step, Fig. 3.

Both release of volatiles and char gasification have important implications for the design of the fuel reactor. Ideally, the fuel will be completely converted to $CO_2$ and $H_2O$ in the fuel reactor. In the case of solid fuels, a fully oxidized gas is normally not attained, which can be remedied by adding oxygen in a post-oxidation chamber downstream of the fuel reactor, so-called "oxy-polishing". Fig. 4 illustrates the three likely deviations from the ideal case; (i) loss of combustible gases like $H_2$, CO and $CH_4$ in the gas leaving the fuel reactor; (ii) loss of char to the air reactor; and (iii) loss of char with the gas leaving the fuel reactor. The corresponding performance indicators are:

i. Oxygen demand, $\Omega_{OD}$, is the oxygen required to oxidize unburnt gas leaving the fuel reactor to $CO_2$ and $H_2O$ over the total oxygen needed to oxidize the gases released from the fuel in the fuel reactor. $1-\Omega_{OD}$ is the gas conversion. The oxygen demand indicates the oxygen needed for oxy-polishing.
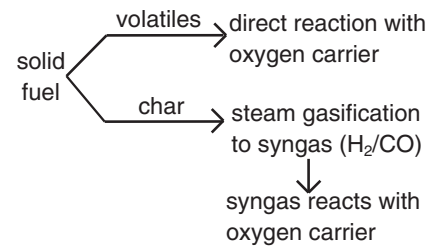
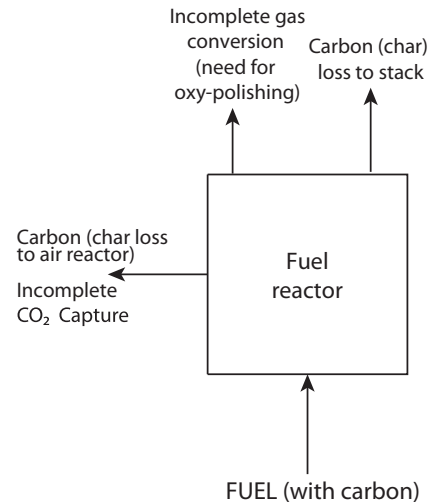ii. $CO_2$ capture, $\eta_{CO2}$, is the fraction of gaseous carbon leaving the fuel reactor related to the total carbon converted to gas in fuel and air reactors. Thus, $1-\eta_{CO2}$ represents the ratio of the carbon lost as $CO_2$ from the air reactor to the total carbon in gaseous compounds leaving air and fuel reactors.

iii. Fuel conversion, $\eta_F$, is used to indicate the char conversion and is defined as the ratio of carbon converted to gaseous compounds in the fuel and air reactors to total carbon added. Consequently, $1-\eta_F$ is the fraction of total carbon added that is elutriated from the fuel reactor in the form of char.

CLC with solid fuels requires a design of the fuel reactor that differs from that of the CLC with gaseous fuels, and oxygen carriers with other properties are preferred:

• The ash, normally being part of solid fuels, reduces the lifetime of the oxygen carrier, as ash removal inevitably results in losses of oxygen carrier. Also, the ash might directly affect the oxygen carrier, indicating the need for a low-cost oxygen carrier.
• The gasification of char is a slow process, and the fuel reactor should be designed to provide sufficient residence time for solids in order to prevent char particles from reaching the air reactor. $CO_2$ produced by char burning in the air reactor is not captured and that should be avoided.
• To achieve high conversion of the volatiles, the fuel should be fed to the fuel reactor in a way that allows good contact between the bed material, i.e. the oxygen carrier, and the volatiles released.

An advantage of CLC operating with solid fuels is that most oxygen carriers, including low-cost materials, are highly reactive towards syngas. However, the syngas is released from char

particles moving around inside the fuel reactor, in contrast to gaseous fuels which are introduced from below. Thus, some of the syngas, particularly that released in the upper regions of the fuel reactor, will have insufficient contact with the bed material. Therefore complete conversion of the gas is difficult to achieve in the fuel reactor. There are several ways to reach full conversion of the gas; in this study, it is assumed that oxy-polishing is used, which means that oxygen is introduced downstream of the fuel reactor in order to oxidize remaining unconverted gases, e.g. $H_2$, $CO$, $CH_4$, $H_2S$ and $NH_3$.

## 2. Operational experience

Total operational experience using solid-fuel CLC amounts to more than 2000 h in eleven units in a size range of 0.5 kW to 3 MW. With the exception of a 25 kW unit using a moving bed fuel reactor [22], they all use fluidized beds. The largest are a 3 MW unit that has been operating with $CaSO_4/CaS$ as oxygen carrier [23]; a 1 MW unit operated with ilmenite [24]; a 100 kW unit with several publications covering operation of various fuels and oxygen carriers, modelling and mass balances; and a 50 kW unit recently taken into operation [25]. The 1 and 3 MW units have both demonstrated autothermal operation. Most of the operation in the pilots involves low-cost iron oxide and ilmenite [2,26]. The operational experience shows that the process works well, but that full conversion of the fuel to $CO_2$ and $H_2O$ in the fuel reactor is normally not attained.

For example, the 100 kW pilot at Chalmers University shows a gas conversion of up to 84% with pulverized coal and ilmenite and considerably higher conversion of up to 95% for low-volatile fuels like wood char [20,27]. The latter illustrates that the conversion of syngas generated from char is high but that the conversion of volatiles is less efficient. Operating this unit has also shown that the overall gas conversion may be significantly improved by adding manganese ore [27]. The $CO_2$ capture in the 100 kW unit, using pulverized coal, was typically around 98%. Thus, partly thanks to a carbon stripper, little char was lost to the air reactor. On the other hand, the fuel reactor experienced a large loss of char with the exiting gases, but as discussed in the section on performance below, this result should have little relevance for larger scale operations.

## 3. Tentative design of a CLC–CFB plant

A CLC power plant using solid fuel would have significant similarities to a CFB power plant, a commercially viable technology for sizes up to 600 MW$_e$. The air reactor could be set up as a CFB boiler, with some notable differences, such as higher solids circulation and smaller gas flow as the oxygen is consumed and no combustion products are released. The gas flow through the fuel reactor is made up by the combustion products $CO_2$ and $H_2O$, typically 20–25% of the total gas flow, and some extra gas added for fluidization. Because the gas flow in the fuel reactor is much smaller than the gas flow in the air reactor, the fuel reactor could be considerably smaller than the air reactor. In addition, the fuel reactor would have to be adiabatic.

In the EU ENCAP project, a first design of a 455 MW$_e$ CLC power plant for solid fuel was made. A comparison to a similar fluidized bed combustion power plant indicated a very low efficiency penalty, <3%, as well as a very low $CO_2$ capture cost, 10 €/tonne of $CO_2$, [28]. The major additional cost was associated with the $CO_2$ compression. However, little detail has been published to make these results available.

Below, a tentative design will be presented to highlight the differences and similarities to conventional large-scale CFB boilers. The basis for the design proposed is 1000 MW$_{th}$, corresponding to around 400 MW$_e$. Whenever possible and reasonable the design similar to existing and known technology, without any pretence that such an approach would always be optimal. Most likely, a fully optimized design would diverge more from the design features of commercial CFBs.

### 3.1. Fuel properties in relation to CLC

If related to the heating value, the stoichiometric air needed for combustion is similar for different coals. Table 1 shows the ratio ($H_i/L_0$) of the lower heating value to stoichiometric air demand for 19 coals, the volatile contents of which vary between 5% and 40%. The average of the ratio is 3.8 MJ/m$_n^3$, and the standard deviation is 0.018. The solid fuels in the table are normalized at a moisture content of 4%. An increase in moisture content to 12% lowers the ratio by 0.029. As shown in the table, many other gaseous and liquid hydrocarbon fuels have similar ratios, whereas the ratio is quite different for CO and $H_2$. This ratio is important not only for the calculation of the air needed for a given power, but also for the calculation of the heat balance in the fuel reactor, which will be highlighted in a following section.

Coal 602 with an $H_i/L_0$ ratio of 3.77 MJ/m$_n^3$ is selected for the present calculations. Its composition is given in Table 2.

### 3.2. Fluidizing velocities and circulation

A fundamental condition for the design is an adequate solids circulation between the air and fuel reactor. Too low a circulation will lead to a high temperature difference between the air and fuel reactor, i.e. a low temperature in the fuel reactor that will slow down the char gasification, thus lowering fuel conversion and $CO_2$ capture. The heat balance in Section 3.5 gives the circulation 5.3 tonne/s, which corresponds to 25.5 kg/m$^2$,s. Normally, the circulation in large circulating fluidized beds is, if known, not published, but there are some data in the literature. According to Yue et al. [30], the circulations measured in large CFB boilers are around 6–10 kg/m$^2$,s at fluidizing velocities in the range 5–6 m/s. These

**Table 2**
Composition of coal 602 in% as received.

| Moisture | Ash | C | H | N | S | O |
|---|---|---|---|---|---|---|
| 4.00 | 8.63 | 72.70 | 4.75 | 1.51 | 1.83 | 6.58 |

**Table 1**
Lower heating value ($H_i$) over stoichiometric air demand ($L_0$) for normal conditions. Coal data from [29].

| Fuel | MJ/m$_n^3$ | Fuel | MJ/m$_n^3$ | Fuel | MJ/m$_n^3$ | Fuel | MJ/m$_n^3$ |
|---|---|---|---|---|---|---|---|
| Coal 101 | 3.83 | Coal 302H | 3.78 | Coal 701 | 3.76 | Petrol | 3.76 |
| Coal 102 | 3.80 | Coal 303H | 3.80 | Coal 702 | 3.78 | Fuel oil | 3.77 |
| Coal 201 | 3.82 | Coal 401 | 3.79 | Coal 802 | 3.80 | Methane | 3.70 |
| Coal 202 | 3.82 | Coal 501 | 3.78 | Coal 902 | 3.79 | Propane | 3.77 |
| Coal 204 | 3.80 | Coal 502 | 3.82 | Wood | 3.71 | CO | 5.23 |
| Coal 301a | 3.80 | Coal 601 | 3.78 | Peat | 3.59 | $H_2$ | 4.45 |
| Coal 301b | 3.80 | Coal 602 | 3.77 | Lignite | 3.74 | C | 3.78 |

numbers differ from those reported by Wu et al. [31], where the circulation in a 300 MW$_e$ CFB boiler operated at 5.4 m/s is 42 kg/m$^2$,s. The circulation chosen for CLC–CFB is approximately an average of these two values from the literature. However, to adopt a conservative approach, we assume that the values in the lower range are the most relevant and that we, compared to a reference CFB, need to increase the circulation by a factor of four. There are several alternatives to attain the circulation needed:

(1) The use of a separate, dedicated riser to move particles to the fuel reactor.
(2) A higher velocity, i.e. a smaller cross-section of the air reactor.
(3) A lower height air reactor.
(4) Smaller particles.

The first alternative, a separate riser, is always a solution and has the advantage of decoupling the fluidization of the air reactor and the global circulation. However, it would add some complexity and cost to the boiler system and other solutions will most likely work as well.

In the second alternative, the relationship between gas velocity and circulation is quite complex. In order to raise the circulation by a factor of four, an increase in velocity by approximately 30% is assumed, whereas a rise circulation by a factor of two would require an increase in velocity by 15%. These results are based on measurements in a 12 MW$_{th}$ CFB in which variations of mass circulation by 1–2 orders of magnitude has been achieved by changes in gas velocity, using three particle sizes [32]. Similar results were obtained in a cold-flow model simulating CLC [33]. However, in the present study we choose not to use increased velocity to reach higher circulation because of the risk for erosion of the heat-transfer wall materials. For the CLC design, there is good reason not to significantly deviate from the practice of commercial CFB boilers in this case.

An important feature of an air reactor in comparison to a CFB is the absence of combustible gases and char that need to be well mixed with the combustion air and gain sufficient residence time to become fully converted. Consequently, there is no need for a certain gas residence time and there is no need for, or advantage of, a high reactor. Moreover, as discussed below, the air reactor requires less cooling surface than the CFB boiler. As internal panel walls or external fluidized heat exchangers can be used to increase heat extraction, there is no need for a high reactor to accomplish the heat transfer. Thus, the minimum height of the air reactor is instead determined by the height of the cyclones and ducts feeding the oxygen carrier to the fuel reactor.

The effect of the reduced height on the circulation of solids is given by the decay constant, describing the exponential decay in solids concentration with height. Measurements in a 12 MW$_{th}$ CFB yielded the decay constant $K = 0.23/(u–u_t)$, where u is the fluidization velocity and $u_t$ the terminal velocity, [32]. With u–u$_t$ in the range of 4–5 m/s, the decay constant becomes around 0.05. Consequently a decrease in air-reactor height of 15 m, as proposed in the design below, doubles the circulation, assuming the data from the 12 MW boiler can be used. The height of the air reactor might be further reduced depending on the design and placing of the cyclone, loop-seal and ducts. It is concluded that a reduced air reactor height is an effective measure to increase the circulation of solids.

The fourth option by which the solids circulation may be increased is particle size. As there is no straightforward simple relationship between particle size and circulation, we use data from a 12 MW$_{th}$ CFB [32] indicating that a doubling of the circulation may be attained by lowering the particle diameter by 10%.

Furthermore, the higher density of an ilmenite oxygen carrier, 3800 kg/m$^3$, compared to a normal bed material in CFB, 2600 kg/m$^3$,

motivates an additional lowering of size. A size reduction of 11% compensates for this increase in density, in the sense that it will keep the Archimedes number constant. In total, a size reduction of 20% is then anticipated. Oxygen carrier materials normally investigated in CLC pilots, 100–200 μm, are somewhat smaller than the particle sizes used in CFBs, 150–300 μm.

In a normal CFB the circulation is also affected by a tapered bottom part as well as the split between primary and secondary air addition. In the CLC–CFB case the situation is different because the oxygen in the air does not react with char or volatile gases but with the bed material. To maximize the contact between air and oxygen carrier, a flat bottom bed and no secondary air would be best in the CLC–CFB case. These two differences have opposite effects on the circulation, and it is assumed that the net effect is small.

The terminal velocity becomes 5% lower because the viscosity of air is 7% higher at the higher temperature chosen, 1020 °C. However, the effect on circulation is minor, with an estimated increase of around 10%.

In conclusion, we assume that lowering the height of the air reactor in combination with some decrease in particle size is sufficient to increase the circulation by a factor of four.

### 3.3. Boiler dimensions and flows

The CFB reference is a 1000 MW$_{th}$ plant with the same cross-section per MW and the same height as the Lagisza 460 MW$_e$ plant; otherwise, the plant is a conventional CFB and equipped with six cyclones. The reference plant has the following dimensions:

- Cross-section (Depth × Width): 11 × 25.5 = 280 m$^2$, height: 48 m.

Based on the $H_i/L_0$ ratio and fuel composition, air and flue gas flows as well as the fluidizing velocity have been calculated for the reference CFB, Table 3. The table shows the assumptions and flows calculated for the reference plant leading to a gas velocity of 5.4 m/s.

The total gas flow in the CLC–CFB plant includes extra gas for fluidization of the fuel reactor, as well as for the fluidization of the loop seals connecting the reactors. On the other hand, it is assumed that the air flow may be reduced by the lower air ratio as compared to a conventional CFB. As a result, the normalized gas flow is 5% smaller in the CLC–CFB case despite the added fluidization flow in the fuel reactor, whereas the actual volume flow of gas in the air and fuel reactors together is 7% higher because of the lower gas density resulting from higher temperature. The flows for the CLC–CFB are provided in Table 4, including additional assumptions for air ratio and the flow used to fluidize the fuel reactor (FR). The temperatures were chosen based on the positive experimental experiences at these temperatures.

Table 5 shows the dimensions and velocities assumed for the reference and CLC–CFB cases. As mentioned, the gas velocities in the fuel and air reactors are chosen to be approximately similar to those of the reference case. Fig. 5 shows these dimensions including a comparison to the reference case. The top sections of the two air reactors are 13 m below the top of the fuel reactor,

**Table 3**
Estimated gas flows, reference CFB.

| | |
|---|---|
| Air ratio | 1.2 |
| Fuel moisture, % | 4 |
| $H_i/L_0$, MJ/m$_n^3$ | 3.77 |
| Air flow, m$_n^3$/s | 318 |
| Flue gas flow (wet), m$_n^3$/s | 367 |
| Flue gas flow at 850 °C (wet), m$^3$/s | 1510 |
| Fluidization velocity, m/s | 5.4 |

**Table 4**
Gas flows CFB–CLC.

| | |
|---|---|
| Air ratio | 1.1 |
| Air flow, $m_n^3/s$ | 292 |
| Flow AR net, $m_n^3/s$ | 236 |
| $CO_2$ flow from fuel, $m_n^3/s$ | 48 |
| $H_2O$ (moisture and combustion) from fuel, $m_n^3/s$ | 20 |
| Fluidization gas FR, $m_n^3/s$ | 20 |
| Total FR, $m_n^3/s$ | 88 |
| Total FR and AR, $m_n^3/s$ | 324 |
| Net flow AR at 1020 °C, $m^3/s$ | 1118 |
| Flow FR at 970 °C, $m^3/s$ | 400 |
| Total flow at 1020/970 °C, $m^3/s$ | 1518 |

and the bottom is 2 m higher, meaning that the difference in height is 15 m in total.

Table 5 shows the wall areas including roof and floor. In addition, there may be wing walls and other internal walls designed to yield the desired temperature of operation. The wall area of the air reactor includes the walls shared with the fuel reactor, which are cooled on the air-reactor side but insulated on the fuel-reactor side. The total wall area of the two air-reactor units is 24% smaller than the corresponding surface in the reference case. However, the higher temperature in the air reactor significantly increases the heat transfer, which means that the CLC unit needs less cooling surface area, which is discussed in a later section.

**Table 5**
Dimensions of CFB and CLC–CFB.

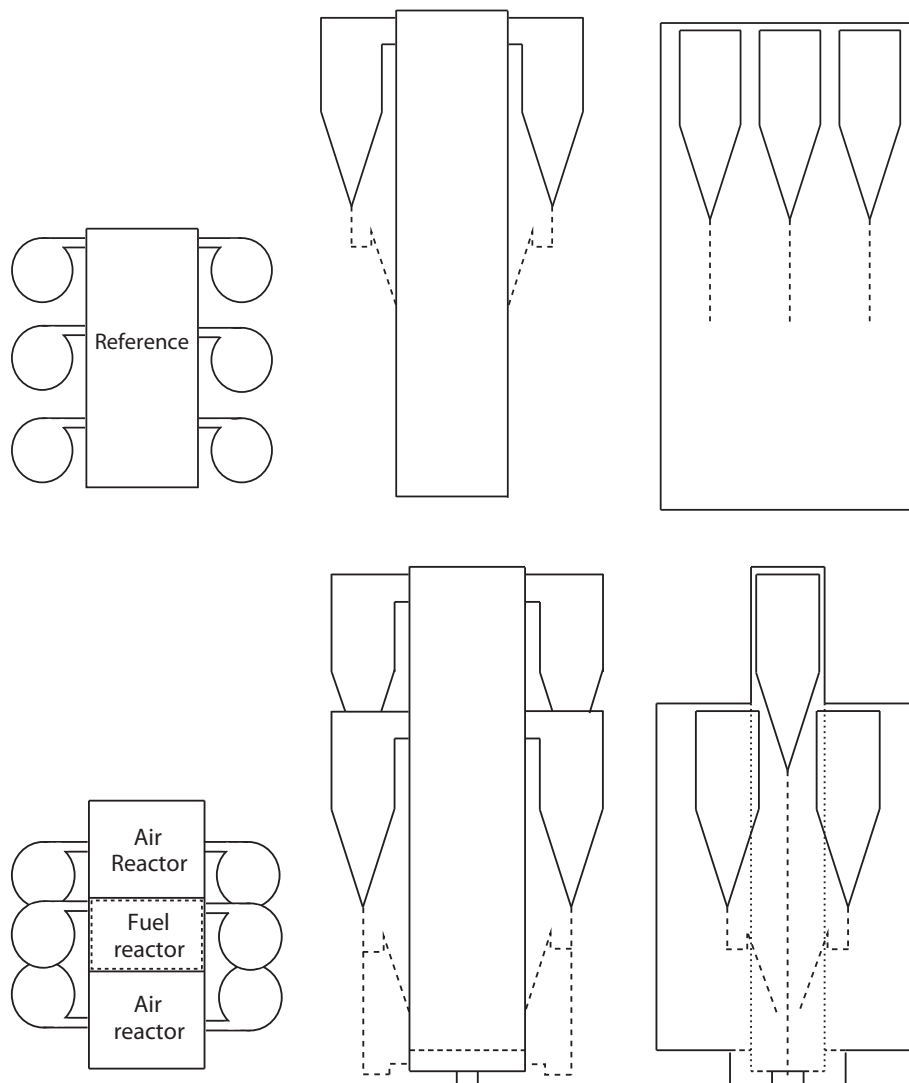| | $D \times W$ | Cross-section, $m^2$ | Gas velocity, m/s | Outer wall area[a], $m^2$ | Inner wall area, $m^2$ |
|---|---|---|---|---|---|
| Reference | $11 \times 25.5$ | 280 | 5.4 | 4227 | – |
| Fuel reactor | $11 \times 7$ | 77 | 5.2 | 1112 | 770 |
| Air reactor | $11 \times 18$ | 198 | 5.6 | 2426 | 770 |
| Fuel + Air reactor | $11 \times 25$ | 275 | – | 3538 | 1540 |

[a] Including roof and floor.



**Fig. 5.** Top, side and front view of reference CFB (top) and CLC–CFB (bottom).

The wall areas of the fuel reactor can be separated into internal walls, i.e. the walls common to the air reactor, and external walls:

- Internal walls, shared with the air reactor: 770 m².
- External walls, including roof and floor: 1112 m².

Both internal and external walls of the fuel reactor are insulated to avoid heat losses. Likewise, the two cyclones of the fuel reactor cannot be cooled and need to be insulated. Assuming an inner diameter of 6 m and a height of 15 m, the two cyclones comprise a total area of 450 m². The total area of ducts leading from and into the fuel reactor is assumed to be 635 m², and an important part of this area belongs to the two tall downcomers from the cyclones of the fuel reactor.

### 3.4. Solids inventories, bed heights and pressure drops

The fuel reactor of the 100 kW Chalmers' pilot has been operated with pressure drops of 14–23 kPa corresponding to 250–400 kg/MW$_{th}$ [34]. A solids inventory of the fuel reactor of 500 tonnes is assumed, i.e. 500 kg/MW$_{th}$. In the case of the air reactor, calculations indicate a minimum solids inventory of 50–100 kg/MW$_{th}$ [35]. A solids inventory of 250 tonnes in the air reactor is assumed. Table 6 shows pressure drops and the defluidized bed heights.

### 3.5. Heat balance and material flows

A convenient way of evaluating the heat balance is to compare the heat produced from the reaction of fuel and oxygen carrier for a given amount of oxygen. The heat of reaction per mole of oxygen for different fuels can be calculated based on the ratio of the heat of reaction to the stoichiometric air, cf. Table 1. Examples of reaction enthalpies for some fuels per mole of oxygen, as well as for some oxygen carriers, are provided in Table 7. It may be observed that the reaction enthalpies of the oxygen carriers are somewhat higher than those of coal. For ilmenite, FeTiO$_3$, it is known that phase separation may occur, leading to the formation of Fe$_2$O$_3$, which should result in a higher reaction enthalpy. A measurement of the reaction enthalpy of ilmenite after 81 h of operation yielded a reaction enthalpy between that of iron oxide and FeTiO$_3$ [36]. This value, i.e. −468 kg/mole, means that for a thermal power of 1000 MW, the heat produced in the air reactor is 1156 MW (cf. the ratio to coal in Table 7) and that the endothermic heat of reaction in the fuel reactor is −156 MW.

Furthermore, energy is used to heat the gas flows and the fuel entering the fuel reactor to the temperature of the fuel reactor. It is estimated that the heating of coal needs 58 MW and the heating of fluidizing gas needs 27 MW.

In addition, the heat loss from the external walls and ducts is assumed to be 1.0 MW and the loss through the internal walls is 0.4 MW. Table 8 shows the heat balance of the fuel reactor. Total heat lost in the fuel reactor is 242 MW. Assuming a temperature difference between the air and fuel reactor of 50 K and a specific heat of the ilmenite of 919.5 J/kg,K yields a required circulation flow of 5.3 tonnes/s. This value was used in the previous section on velocities and circulation. With the inventories given, this circulation flow corresponds to residence times of 95 and 47 s in the fuel and air reactors. Moreover, with a total oxygen transfer of 78.5 kg/s, $\Delta\omega$, the mass-based conversion of the oxygen carrier, is 1.5%, a reasonable value as the oxygen transfer capacity of ilmenite is well above this other figure.

The heat balance assumes full conversion in the fuel reactor. The effect of incomplete conversion can be estimated by comparing the reactions in Table 7. Incomplete conversion would not alter the rate of fuel addition, because gas or char not converted in the fuel reactor is either converted in the air reactor or in an oxygen polishing step downstream of the fuel reactor. Thus, the thermal power is not affected by incomplete conversion in the fuel reactor. Table 9 shows the effect on the heat balance, given the assumptions that 10% of the carbon added leaves the fuel reactor as char, i.e. carbon, 6% as CO, 3% as CH$_4$ and that the hydrogen flow equals the CO flow. Here, the unconverted gas composition assumed would correspond to an oxygen demand of approximately 10%. Unconverted CO and H$_2$ will have a negative effect on the heat balance, because the reaction with the oxygen carrier is exothermic. For the assumed gas composition this effect is compensated for by unconverted CH$_4$ as this avoids the endothermic reaction with the oxygen carrier. Unconverted char will have a similar positive effect on the heat balance. The overall effect in this example is a small reduction of the heat loss in fuel reactor, i.e. from 242 MW to 228 MW. Therefore, it can be concluded that incomplete conversion would only have a minor effect on the heat balance of the fuel reactor.

### 3.6. Bed pressure drop in AR and fluidization of FR with steam and hot CO$_2$

The pressure drop in the AR is 16 kPa, Table 6, which is assumed to cause an added pressure drop for the air fan of 10 kPa compared

**Table 6**
Solids inventories of air and fuel reactors.

|  | Fuel reactor | Air reactor |
|---|---|---|
| Inventory, tonnes | 500 | 250 |
| Pressure drop, kPa | 64 | 16 |
| Settled bed height, m | 3.1 | 0.8 |

**Table 7**
Heat of reaction for oxidation of oxygen carriers and fuels.

| Reaction | $\Delta H$, kJ/mole (O$_2$) | Ratio to coal |
|---|---|---|
| O$_2$ + ½CH$_4$ → ½CO$_2$ + H$_2$O | −401.7 | – |
| O$_2$ + 2CO → 2CO$_2$ | −562.8 | – |
| O$_2$ + 2H$_2$ → 2H$_2$O | −498.5 | – |
| O$_2$ + C → CO$_2$ | −403.3 | – |
| O$_2$ + coal → xCO$_2$ + yH$_2$O | −405.1 | 1 |
| O$_2$ + 4Fe$_3$O$_4$ → 6Fe$_2$O$_3$ | −479 | 1.182 |
| O$_2$ + 4FeTiO$_3$ → 2Fe$_2$TiO$_5$ + 2TiO$_2$ | −445 | 1.098 |
| O$_2$ + ilmenite (from [36]) | −468 | 1.156 |
| O$_2$ + 6MnO → 2Mn$_3$O$_4$ | −449 | 1.108 |

**Table 8**
Heat balance fuel reactor.

|  | Heat, MW |
|---|---|
| Reaction | −156 |
| Heating coal | −58 |
| Heating fluidizing steam | −27 |
| Loss external walls | −1.0 |
| Loss internal walls | −0.4 |
| Total | −242 |

**Table 9**
Effect of incomplete conversion.

|  | Heat, MW |
|---|---|
| Carbon | 13.6 |
| CO | −6.0 |
| H$_2$ | −1.9 |
| CH$_4$ | 8.4 |
| Sum | 14.1 |

to the pressure drop of the primary air of the reference plant. The secondary air in the reference plant will be added through the bottom bed air-nozzles in the CLC–CFB case which is assumed to give an additional pressure drop of 20 kPa. With a ratio of secondary to primary air of unity, this totally adds up to an additional compression work of approximately 4.6 $MW_e$. However, the major part of the electric energy enters the air reactor as sensible heat, and this heat produces an additional 1.8 MW of electricity. Thus, the efficiency penalty for the added pressure drop is somewhat below 0.3%.

For the assessment of the effect of the fluidization of the fuel reactor it is assumed that 1.5 bar steam is used, which is produced by bled steam taken at 2 bar. If only steam were used for fluidization of the fuel reactor, the resulting efficiency penalty would be approximately 0.8%. It is clear that steam for fluidization is critical to the performance and should be minimized as far as possible.

From an efficiency point of view, fluidization with recycled $CO_2$ is preferred. $CO_2$, however, is a poor gasification agent. A better option would be to recycle "hot $CO_2$", i.e. flue gas withdrawn before condensation containing both $CO_2$ and $H_2O$. The efficiency penalty for using "hot $CO_2$" is smaller, estimated at below 0.2%.

In this work, 50% hot $CO_2$ and 50% steam were chosen, which yields a penalty of 0.5% and a steam fraction in the flue gas of 39%. A notable difference between the gasification in a CLC unit and normal gasification is that the steam is not consumed because the hydrogen formed is rapidly re-oxidized to steam. Similarly, the hydrogen in the volatiles also forms steam which becomes available for the gasification.

The above gives a total energy penalty for fluidization of the air and fuel reactors of approximately 0.8%, which is estimated to yield a $CO_2$ avoidance cost of approximately 0.8 €/tonne $CO_2$.

### 3.7. Fuel reactor connections and design

Normally, the flow of solids from the cyclones is returned above the bottom bed. In the case of CLC, feeding the material from the cyclone of the fuel reactor low down into the bed is motivated by a desire to reach a high conversion of char, as one important purpose of the cyclone is to separate unconverted char and return it to the fuel reactor. Furthermore, feeding fuel into this return flow would help to introduce the fuel into the fuel reactor. A consequence of returning the material in the bottom bed is that there is a high particle column in the standpipe of the downcomer from the cyclone. To avoid production of gas that might disturb the cyclone operation, the loop seal should be fluidized by $CO_2$.

As noted in Table 4, the major gas flow in the fuel reactor comes from the oxidation of gases formed by the fuel through devolatilization and gasification. The remaining part of the gas flow is the gas necessary to assure that the bed is properly fluidized over the entire cross-section. This flow is 20 $m_n^3/s$ or 23% of the total gas flow in the fuel reactor, corresponding to a fluidizing velocity of around 1 m/s in the lowermost part of the bed.

In order to avoid a local plume of volatiles where fuel is added without having to resort to a large number of fuel entries, a device for distributing volatiles is used. The principle of such a "volatiles distributor" is described in a patent application [37]. It is based on the fact that a box immersed in a fluidized bed with the opening downward would become empty, which means the bed surface would follow the lower edge of the box. If such a box had any openings, the bed surface would rise to the level of the openings. In short, the volatiles distributor can be described as an elongated box with the opening downward and holes on the sides. If this distributor is immersed in a fluidized bed, the bed material would form a bed surface at the level of the holes. Above this surface, gas can flow freely and gas injected into this distributor would leave the distributor via the holes. The fuel should be added in such

a way that the volatiles are released in a gas volume connected to the distributor. Furthermore, the volatiles distributor would have a number of "arms" to assure a good distribution of volatiles across the cross-section.

A possible lay-out of such a volatiles distributor and its placement at the bottom part of the fuel reactor is provided in Figs. 6a–6c. The detailed design would need to be optimized, using experimental data from cold-flow testing in combination with fluid-dynamic modelling, as well as cost analysis. Considering the conditions in the fuel reactor, such a construction would likely have a limited lifetime, making regular replacements necessary. Nevertheless, the volatiles distributor is worthwhile, considering the importance of good contact between the reacting gas and oxygen carrier to achieve high gas conversion with the aim of minimizing oxygen production for polishing.

Figs. 6a and 6b shows how the material is returned from the cyclone of the fuel reactor, and how the fuel is added to the freeboard on the downstream side of the loop seal. Fuel added follows the flow of solids coming from the cyclone of the fuel-reactor. The material coming from each downcomer is divided into two flows. The freeboard where the fuel is added, Figs. 6a and 6b, is extended to form a channel which goes all along the external wall of the fuel reactor. This channel connects to the arms of the volatiles distributor and could be used for additional fuel entries. Determination of
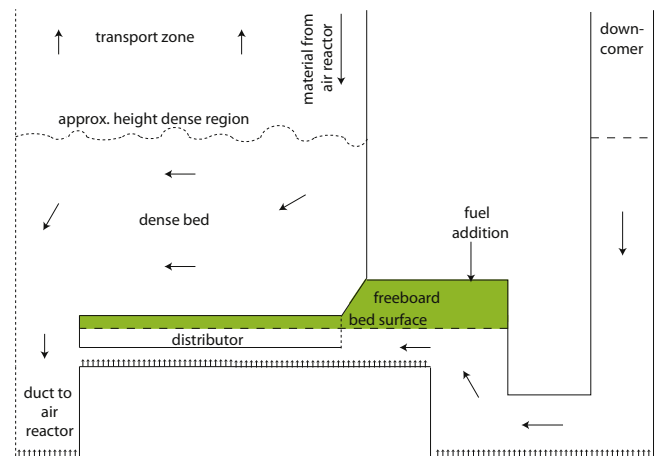
**Fig. 6a.** Side view of the right-hand half of the fuel reactor showing volatiles distributor and solids return. Arrows indicate movement of bed material.
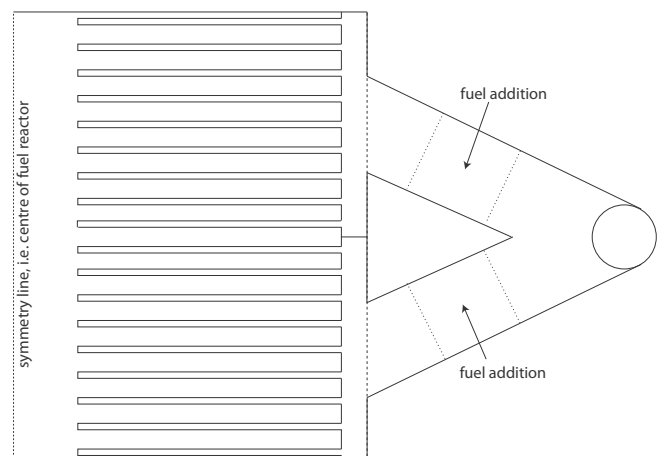
**Fig. 6b.** Top view of the right-hand half of the fuel reactor, showing volatiles distributor and solids return.
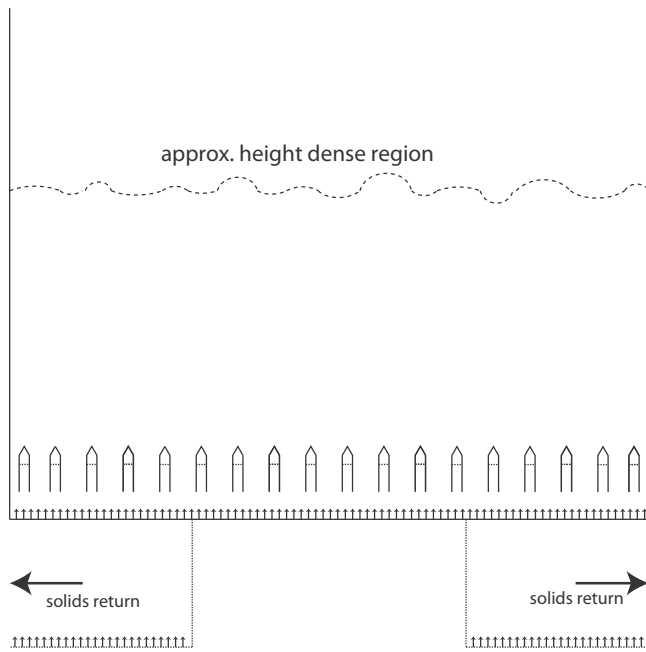
**Fig. 6c.** Other side view showing cross-sections of the arms of the volatiles distributor and solids return to the air reactor.

the optimal locations and number of fuel inlets into the freeboard connected to the distributor requires detailed studies.

Most of the gas going through the fuel reactor is generated in the bed. Assuming that the fuel char has similar distribution versus height as the bed material and that the volatiles are all released from the volatiles distributor, it is possible to estimate the gas flow versus height, Fig. 7. The gas velocity is low in the bottom part and increases linearly in the dense zone, except at the level of the volatiles distributor where the velocity increases stepwise.

The volatiles distributor would be made from expensive high-temperature steel, e.g. 253MA, and would need to withstand the forces of a fluidized bed. A thickness of 20 mm is assumed which translates to approximately 21 tonnes of steel. It is assumed that a large number of legs is needed to keep the structure stable, resulting in 30 tonnes of steel in total. An assumed price of 2000 €/tonne together with a life of only one year gives a material cost of 60,000 €, or 0.03 €/tonne of $CO_2$. This cost is small and omitted in the calculations below.
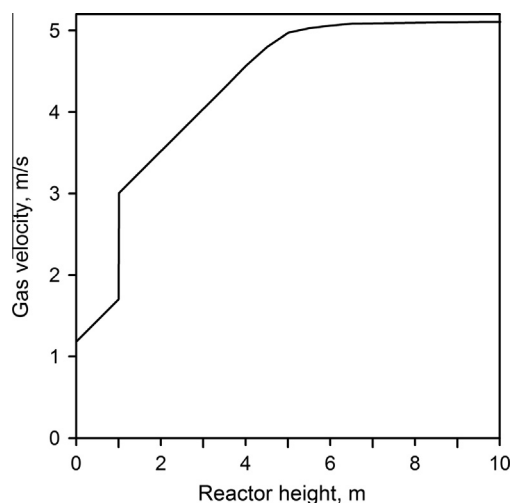


**Fig. 7.** Gas velocity in fuel reactor versus height.

There are several ways of organizing an exchange of oxygen carrier between air and fuel reactors, as is obvious from the smaller CLC pilots. Here, it is assumed that the material flows from the two air reactors, see Fig. 5, are conveyed to the fuel reactor via the cyclones of the air reactors and enter the fuel reactor above the denser bottom zone. As there are four cyclones, the material enters at two locations on each external wall, for instance above the entries of the recycled material. The flows of solids coming from the air reactors are much greater than those from the cyclones of the fuel reactor. In order to achieve a reasonably good residence-time distribution, the oxygen carrier is removed from the fuel reactor at a point far away from the inlet, at the bottom of the centre line. From here, the material is transferred to the air reactor via a loop-seal that directly connects the air and fuel reactors, using the same principle as in the Vienna 100 kW CLC [38].

The air and fuel reactors operate with significantly different bed heights, see Section 3.3, and such a connection means that the bottom of the air reactor should be elevated compared to the fuel reactor by a little more than 2 m.

### 3.8. Heat transfer surfaces

In order to assess the effect of the increased temperature in the air reactor on the heat exchanger area, a wall temperature of 400 °C is assumed. It is assumed that radiation dominates. The radiative heat transfer is proportional to the temperature difference between the bulk particles, $T_1$, and the wall, $T_2$, and the effective heat transfer coefficient, $\alpha$

$$\frac{P}{A} = \alpha(T_1 - T_2) \tag{1}$$

where $\alpha$ is

$$\alpha = \eta \varepsilon_{res} \sigma (T_1 + T_2)(T_1^2 + T_2^2) \tag{2}$$

where $\sigma$ is Stefan-Bolzmann's constant, $\varepsilon_{res}$ is the resulting emissivity and $\eta$ is the radiative efficiency to account for the particle wall layer. The effect of increased temperature difference, for a temperature increase from 850 °C in the CFB to 1020 °C in the CLC–CFB, is an increase in the radiative heat transfer of 87% corresponding to a reduction in heat transfer surface of 46%. The result is not very sensitive to the assumption of wall temperature, and assuming 300 or 500 °C instead would only change the heat transfer surface by a few per cent. Thus, we assume a reduction in heat transfer surface of 45–50%.

In the convection pass, the radiative heat transfer is minute and gas convection dominates. Therefore, any effects on the heat transfer in the convection pass are neglected here.

We assume that the reduction in heat transfer area is 990 m$^2$ and the specific cost is 3300 €/m$^2$, providing a cost reduction of 0.17 €/tonne of $CO_2$ using the costing data in Table 10

### 3.9. Cost of fuel reactor and post-oxidation chamber

Fig. 5 shows that the fuel reactor replaces part of the reference CFB. Nevertheless the walls of the fuel reactor are associated with an added cost, since the walls need to be well insulated and do not contribute to the heat transfer. For internal walls with a thickness of lining of 100 mm, a cost of 900 €/m$^2$ is assumed, giving a total cost of 0.7 M€.

**Table 10**
Basis for cost difference calculations.

| | |
|---|---|
| Yearly depreciation | 10% |
| Yearly full-load operational time | 6000 h |
| $CO_2$ capture | 98% |

The oxygen for post-combustion, i.e. oxy-polishing, can be added to the cyclone outlet pipe to take advantage of mixing the gas into the swirl. The gas then enters an adiabatic duct, assumed to have a volume of 200 $m^3$ to be sufficient for complete combustion, corresponding to a residence time of 0.5 s. With a duct diameter of 4 m, the length of each of the two ducts from the two cyclones of the fuel reactor is 8 m. The wall area becomes 250 $m^2$. Assuming similar length of the ducts and a residence time of one second, the diameter would increase to 5.6 m and the area would increase by 130 $m^2$.

The total external insulated area, including the external walls of fuel reactor, ducts, cyclones, and post-oxidation chamber, becomes 2447 $m^2$. The cost of a 400 mm insulated wall is assumed to be 1500 €/$m^2$ giving a cost of 3.7 M€. The most uncertain cost is that of the area of the post-oxidation chamber. A doubling of the residence time in this chamber, however, increases the total surface by less than 10%.

The total added cost of insulation of the fuel reactor, ducts and post-oxidation chamber, with the costing data of Table 10, is 0.22 €/tonne of $CO_2$.

In this cost, all walls/surfaces of the fuel reactor as well as cyclones, ducts and post-oxidation chambers are included. However, all of these surfaces are not added costs in reality, as some of these costs relate to cyclones and ducts already available in the reference CFB. Thus, the number is conservative and implies some overestimation.

In total, the change in boiler cost, including added insulated walls and reduced heat transfer surfaces, amounts to around 0.05 €/tonne of $CO_2$.

Another approach to assess costs related to the boiler is to assume relative cost changes. In this case, we make the alternate assumption that the modifications and adaptations of the boiler for CLC give a significant overall cost increase that has not been captured by the estimations performed in this study, and that these costs correspond to a boiler cost increase of 15%. Furthermore, we assume that the investment cost of the reference plant is 1200 €/$kW_e$, and that the boiler island constitutes 25% of this cost. Using the costing data in Table 10, we find that the assumption of a 15% increase in boiler cost corresponds to a $CO_2$ capture cost of 2.3 €/tonne of $CO_2$.

## 4. Ash removal

The separation of ash and oxygen carrier in the mixed effluents from the boiler is a key issue. In normal CFBs, an important part of the ash consists of larger particles leaving as bottom ash, although most ash comes out as fly-ash. An important difference between the two cases, however, is the size of the fuel used in CFBs, typically 1–6 mm, while in the CLC–CFB case, the particle size needs to be much smaller. Assuming that pulverized fuel is used, the fuel particles have a $d_{50}$ of around 60 μm. Then the ash particles formed will be even smaller, considerably smaller than the oxygen carrier particles, and leave the process as fly-ash. Nevertheless, some regeneration of the bed material may be needed to avoid ash accumulation.

Most fuel ash leaves the system from the fuel reactor. In particular, a loss of oxygen-carrier material from the cyclones of both air and fuel reactors can be expected, not only fine particles from attrition, but also larger particles desirable for recovery and recycling. These particles are separated from the gas flow by filters together with the ash particles. The larger gas flows from the air reactor could be assumed to contain mainly oxygen-carrier particles that could be recycled. The gas flows from the fuel reactor, however, also contain fuel ash and char not burned in the post-oxidation chamber. Perhaps it would be worthwhile to separate these oxygen

carrier particles from the ash by magnetic separation to reduce the loss of oxygen carrier. Oxygen carrier materials like ilmenite, iron ores and manganese ores could be expected to be sufficiently magnetic for such separation.

It is possible that ash compounds interact with the oxygen carrier causing slow aging. This is dependent on the ash characteristics and may have implications for the selection of fuel.

## 5. Additional costs

### 5.1. Fuel grinding

The CLC process uses a smaller fuel size than normal fluidized-bed combustion of coal. The coal size will be the result of an optimization based on the following factors:

- Larger fuel particles reduce the loss of char fines elutriated with the exit gas and lower the oxygen needed for oxy-polishing.
- Larger fuel particles reduce the power need for grinding.
- Smaller fuel particles reduce the loss of char fines to the air reactor, which improves the $CO_2$ capture.
- Smaller fuel particles result in smaller ash particles, which are more easily elutriated giving more fly-ash and less bottom ash. This fact facilitates the overall separation of ash and oxygen carrier, leading to a longer life for the oxygen carrier.

The milling of the fuel is assumed to consume 10 kWh/tonne fuel, or 1 MW, and thus reduces the efficiency by 0.1%, which corresponds to a cost of around 0.1 €/tonne $CO_2$. The added cost for milling equipment is uncertain but is assumed to be 0.1 €/tonne $CO_2$, giving a total of 0.2 €/tonne $CO_2$.

### 5.2. Loss of unconverted char

It is assumed that any char lost from the fuel reactor is burned in the post-oxidation chamber. Lost char then adds to the oxygen demand.

### 5.3. Reduced flue gas loss

The lower air ratio for CLC is estimated to increase the overall efficiency by 0.5%, giving a negative cost of −0.5 €/tonne $CO_2$.

## 6. Expected performance

### 6.1. Fuel conversion

The fuel conversion in the 100 kW unit is compromised by a significant loss of elutriated char leaving the system via the cyclone. However, the cyclone efficiency of the 100 kW unit is poor, probably because of the significant pressure fluctuations caused by the slugging of the bed, and a full-scale cyclone operated under normal conditions could be assumed to have better separation. Furthermore, the large-scale fuel-reactor is approximately ten times higher, which significantly increases the time for a char particle to travel from the bottom to the top of the reactor. If we combine this with a significantly improved cyclone efficiency, the actual residence time of a char particle before it is lost from the cyclone, increases by orders of magnitude. Consequently, the loss of unconverted char is dramatically reduced in a full-scale unit as compared to the 100 kW pilot. Lastly, unconverted char may burn in the post-oxidation chamber or be captured in filters and returned to the fuel reactor. At this stage, it is difficult estimate the fuel conversion in the full-scale plant, but it is assumed to be

97% in the fuel reactor and 100% in total, i.e. all char lost burns in the post-oxidation chamber.

An option might be to design the post-oxidation chamber as a secondary cyclone, both separating char particles and increasing their residence time, as well as contributing to gas mixing.

### 6.2. Gas conversion

The analytical model previously used for the 100 kW unit [34] yields a gas conversion of 93–94% for the 1000 MW CLC–CFB employing the same data for ilmenite reactivity, composition of volatiles and factors describing the imperfect contact between gas and solids. This is a significantly higher conversion than in the 100 kW unit, where it is 84% at best. The improvement is partly caused by the assumption of higher char conversion, $\eta_F$ = 97%, and by a slightly larger bed mass per $MW_{th}$, but the most important difference is the much lower dilution of the gas flow by the fluidizing gas. In the 100 kW unit, the gas is diluted with higher additional gas flows for fluidization, as well as by the gas flows from the loop seals and the fuel feed system.

The results from the 100 kW unit were obtained with ilmenite and bituminous coal; a significantly higher gas conversion is attained in operation with manganese ore or low-volatile fuels.

Furthermore, it is clear that the 100 kW unit operates in the slugging mode, which is a consequence of the scale: a small riser diameter and a high bed inevitably lead to slug formation resulting in poor contact between gas and solids. In the model, the contact factor for the volatile conversion used is 0.15, which means that the model assumes that only 15% of the solids are in contact with the gas. Slugging would not occur in a full-scale unit, and, besides, the fluidization velocity would be much higher. Therefore, the gas contact is probably better and the gas conversion is further improved.

### 6.3. Oxygen need

From the model results suggesting a gas conversion of 93–94%, we assume an oxygen demand for the gas of 7%; to this we add the need for oxygen demand for char burn-up, yielding a total oxygen demand of 10%. This number is uncertain as there are many factors that may influence the oxygen need, but in view of the likely improvements from adding manganese ore, it is expected that the total oxygen demand should be in the range 5–15%.

### 6.4. CO₂ capture

The 100 kW unit includes a carbon stripper and is able to reach a CO₂ capture of 98%. The 1000 MW$_{th}$ unit does not have a similar dedicated carbon stripper; Because the exit of the bed material at the bottom of the bed is more than 5 m from the fuel feed location, the fuel reactor itself will work as a carbon stripper. The transport distance will provide some time both for conversion and stripping of char particles, the latter separation mechanism caused by char fines moving upwards with the gas flow. Consequently, it is assumed that a similar CO₂ capture, i.e. 98%, can be reached for the 1000 MW$_{th}$ unit without an actual carbon stripper.

If further enhanced separation is needed, it is possible to extend the connection between fuel and air reactors downwards. This option would involve some minor additional costs for insulated walls and steam of higher pressure for the fluidization of this part.

## 7. Oxygen carrier cost

Because of the uncertainties in the lifetime of the oxygen carriers in actual operation, the selection and cost of the oxygen carrier

**Table 11**
Examples of CO₂ capture costs related to oxygen carrier materials.

|  | Ilmenite | Manganese ore |
|---|---|---|
| SE, tonne/MWh$_{th}$ | 0.334 | 0.334 |
| SI, tonne/MW$_{th}$ | 0.75 | 0.75 |
| $\eta_{CO_2}$ | 98% | 98% |
| $\tau$, h | 200 | 100 |
| $C_{OC}$, €/tonne oxygen carrier | 175 | 225 |
| CCC$_{OC}$, €/tonne CO₂ | 2.0 | 5 |

are very important. Clearly, low-cost natural minerals or waste materials are advantageous. While the price of ores, metals and oxides vary from year to year, current prices are in the range 200–250 €/ton for manganese ore, around 150–200 €/ton for ilmenite and even lower for iron ore.

The cost of oxygen carrier adds to the CO₂ capture cost. The cost for the oxygen carrier can be expressed as the cost per tonne of CO₂ captured and is given by

$$CCC_{OC} = \frac{C_{OC} \cdot SI}{SE \cdot \eta_{CO_2} \cdot \tau} \qquad (3)$$

where CCC$_{OC}$ is the Cost of CO₂ Capture caused by the Oxygen Carrier in €/tonne CO₂ captured, $C_{OC}$ is an estimated cost of oxygen carrier in €/tonne, SI is the solids inventory in ton/MW$_{th}$, SE is the specific emission of the fuel in tonne CO₂/MWh$_{th}$ and $\tau$ is the average lifetime of the oxygen carrier. A pilot operation using ilmenite suggested a life of 600–700 h [21] based on the production of fines. This lifetime estimation does not consider any interaction with ash, and a more realistic lifetime is probably 100–300 h. With ilmenite and assuming a lifetime of 200 h, the cost is 2 €/tonne CO₂, Table 11. Consequently, a lifetime of 100–300 h yields a cost range of 1.3–4 €/tonne CO₂.

For manganese ore, a shorter lifetime based on present limited experiences is assumed, leading to a higher estimated cost for manganese ore of around 5 €/tonne CO₂.

## 8. Compression and oxygen production

The compression of carbon dioxide involves costs for equipment and operation as well as a significant energy penalty of around 3%. The energy penalty is defined as the reduction in percentage units of the overall efficiency of a power plant, for instance from 43% to 40%. Such a compression is needed for all CO₂ capture processes, and the cost and energy penalty for compression is normally estimated to be much lower than that of the actual capture, i.e. attaining a stream of CO₂ ready for compression. A cost of 10 €/tonne of CO₂ is assumed for compression, including the costs of the energy penalty and gas treatment.

The boiler costs differ from that of a conventional boiler despite the many similarities to the reference CFB case. While the air reactor is very similar to a CFB, the major difference is the added cost of the adiabatic fuel reactor and its post-oxidation chamber. However, an estimation of these added costs indicates that the change in cost is minor, cf. Section 3.9.

In view of the many similarities to oxyfuel combustion, we can make a comparison to this process. It is assumed that oxyfuel combustion has a total cost of 50 €/tonne of CO₂, which involves CO₂ compression, 10 €/tonne, and air separation, 40 €/tonne. Downstream treatment, e.g. SO₂ and NO$_x$ removal and CO₂ purification is included in the compression cost. The added costs for the downstream treatment are assumed to be moderate because conventional SO₂/NO$_x$ removal can be avoided and the removal of SO₂/NO$_x$ in a much smaller gas stream and at a higher concentration can be expected to be less costly. Compression and air

separation both have significant energy penalties, which means that these costs include larger power plant investment and operating costs, such as fuel, per unit of electricity produced.

In the CLC–CFB case, it was estimated that the amount of oxygen needed for oxy-polishing is 5–15% of the total oxygen requirement. The specific cost of air separation is higher because of smaller flows. Using the assumption above for oxyfuel but assuming that the air separation cost is proportional to the amount of oxygen raised by a power of 0.8 to express the scale effect, a cost of air separation of 4–9 €/tonne is obtained, i.e. a reduction by 77–90% compared to oxyfuel.

Downstream treatment involves removal of $SO_2$, $NO_x$, argon, fuel-$N_2$, excess oxygen and air from ingress. CLC–CFB differs from the oxyfuel case in some respects. Firstly, the argon to be separated is an order of magnitude smaller, as much less oxygen is used for the oxy-polishing. Secondly, the gas flow from an oxyfuel boiler, before $CO_2$ recycling, is much larger than the flow from the fuel reactor. This might make it easier to avoid air ingress. Presently, it is not clear whether CLC–CFB yields more or less $NO_x$ as compared to oxy-fuel combustion. On the whole, however, it is likely that the costs of $CO_2$ purification are similar or somewhat lower as compared to oxy-fuel.

## 9. Total costs

The total estimated added costs and energy penalties for a CFB–CLC are provided in Table 12.

In summary, it is clear that the main costs are $CO_2$ compression including gas treatment and oxygen production for the oxy-polishing. Both of these costs are also being investigated in connection with other $CO_2$ capture technologies, oxyfuel combustion in particular. The focus in this study is on the costs directly related to chemical-looping, as it was not the purpose to investigate the costs of compression and oxygen production, and therefore they are only assumed. Nevertheless, these two costs are the main part of the total costs. The analysis is transparent and allows for corrections of the costs presented and any numbers can be improved as more detailed and accurate information becomes available.

The cost relations between oxygen carrier and oxy-polishing are helpful in the selection of oxygen carrier materials, as they can be used to estimate whether a more reactive and more expensive oxygen carrier might result in lower costs.

## 10. Discussion

### 10.1. The high bed in the fuel reactor

The bed in the fuel reactor is much higher than what is normal practice in CFB boilers. However, above a certain amount, the bed inventory in tall reactors is not decisive for the overall behaviour of the solids. With respect to solids inventory Hu et al. [39] have shown that in tall risers, in their case 38 and 54 m, the particle flow

**Table 12**
Estimated added costs for CFB–CLC.

| Type of cost | Estimation, €/tonne $CO_2$ | Range, €/tonne $CO_2$ | Efficiency penalty, % |
|---|---|---|---|
| $CO_2$ compression | 10 | 10 | 3 |
| Oxy-polishing | 6.5 | 4–9 | 0.5 |
| Boiler cost | 1 | 0.1–2.3 | – |
| Oxygen carrier | 2 | 1.3–4 | – |
| Steam and hot $CO_2$ fluidization | 0.8 | 0.8 | 0.8 |
| Coal grinding | 0.2 | 0.2 | 0.1 |
| Lower air ratio | −0.5 | −0.5 | −0.5 |
| Total | 20 | 15.9–25.8 | 3.9 |

saturates if the solids inventory is high enough, which is definitely fulfilled in the present case and does not change with additional inventory. Even though the local behaviour of the flow, particularly in the lower part of the reactor, is affected by the solids inventory, the overall performance including the resulting solids flow is not affected, provided that the bed is not starved. A criterion for a (non-slugging) reactor not to be starved is that a bottom bed remains, while the fluidization velocity is above the transport velocity, which is the case in all risers concerned here. Of course, as has been pointed out above, circulation of solids is influenced by fluidization velocity and particle properties.

### 10.2. A clean air-reactor gas

There will be a small loss of char from the fuel reactor to the air reactor, which is converted to $CO_2$ in the air reactor. Furthermore, nitrogen and sulphur present in this char form minute amounts of $SO_2$ and NO. Only a small amount of fuel ash is expected to reach the air reactor. Consequently, the gas in the air reactor will be comparatively clean, with concentrations of combustible products being almost two orders of magnitude lower than in conventional flue gas. This situation is in contrast to a CFB boiler having not only much higher concentrations of $CO_2$, $H_2O$, $SO_2$ and $NO_x$ compounds, but also local releases of volatiles containing reducing and reactive gaseous compounds like $H_2$ and $H_2S$. The absence of such compounds and the low concentration of water vapour could be an advantage for the corrosion resistance of the heat exchanger surfaces.

### 10.3. Control of solids circulation

It is crucial that the plant is designed to make the needed circulation possible. But it is also necessary to have some option to control the global circulation: a CLC power plant must not be built without any option to control global circulation as this is a key parameter for reaching the desired operating conditions. Too low a circulation would lower the temperature of the fuel reactor and too high a circulation will compromise the desired residence time of the solids in the fuel reactor, thus lowering carbon capture. Therefore, some options to control circulation are briefly mentioned:

- The main option in normal operation is to control the particle size. As noted above, the circulation is sensitive to particle size. However, the control of particle size involves the streams of solids entering and exiting the system, and can be expected to respond slowly to corrective measures. Options for controlling the circulation should also involve measures with more immediate response.
- One way to rapidly increase circulation would be to raise the gas velocity in the air reactor by the addition of recycled oxygen-depleted air in the form of secondary air.
- Another possibility is to design the unit with some excess circulation, but without sending the full flow to the fuel reactor. This can be done by diverting a part of the circulation flow back to the air reactor using controllable loop-seals with double exits [40].

### 10.4. Part load operation

The possibility to operate a power plant at partial load is important and expected to become even more important with increasing production of power from wind and solar energy. As this will inevitably become a key issue in the design of future power plants, it will be briefly discussed here.

In chemical-looping combustion it is impossible to significantly reduce the gas velocity in the air reactor, because that would stop the solids circulation. However, there are two ways to vary the load, either through a separate system for solids circulation, which is independent of the air flow to the air reactor, or by partitioning of the air reactor.

In the design proposed, there are two air reactors, opening up the possibility of switching between a load of 100% and 50%. One air reactor can be defluidized while the other is operated normally. The consequence for the fuel reactor is a lowered gas velocity and a doubled solids residence time. In general, longer gas and solids residence time is beneficial for the conversion of gas and char. However, the reduction in gas velocity would significantly reduce the solids circulation passing through the cyclone of the fuel reactor, which might lead to difficulties with the flow in the downcomer and loop seal, particularly if the fraction of char fines were to become dominant.

One option would be to inject recycled "hot $CO_2$". Assuming a temperature of 235 °C, and an addition large enough to give the same velocity as at full load, the heat balance of the fuel reactor would be significantly altered. This change in heat balance means that the global circulation needs to be increased by 53%, or that the temperature difference between the air and fuel reactor increases from 50 to 77 °C. The best alternative would probably be a combination of (i) having lower velocity but adding sufficient hot $CO_2$ to give adequate operation, (ii) some increase in the global circulation, (iii) accepting a somewhat lower fuel reactor temperature. With respect to (ii) there are some options for circulation control as discussed in the previous section.

### 10.5. Risks in upscaling

The greatest barrier to the development of CLC–CFB technology is that it does not make sense in the small or intermediate scale. Also, with the climate issue becoming more pressing, it is important to move quickly towards a larger scale, possibly by an intermediate step of 30–100 MW$_{th}$. Consequently, the gradual increase in boiler size typical of the development of CFB technology over the past 30 years would need to be made in larger steps during the development of CLC–CFB technology, which evidently involves risks. However, the similarities and experiences of CFB technology is an advantage in the development of the CLC–CFB technology. Technology risks and possible mitigations are summarised below.

- Inadequate performance of the oxygen carrier. A number of low-cost oxygen-carriers can be to used, including ilmenites, manganese ores and iron ores. For these materials, there is a large market with many possible suppliers. Operation in smaller pilots indicates that these materials are sufficiently reactive. However, aging of materials might be an issue with the consequence of higher oxygen carrier costs.
- Inadequate solids circulation. If operational measures like reduced particle size are not sufficient or possible, it might be necessary to add dedicated circulation risers. These risers would be adiabatic with cyclones leading the solids to the fuel reactor. They would be small in comparison to the fuel reactor and, consequently, the added cost should be moderate.
- Difficulties with a high solids inventory in the fuel reactor. The high bed proposed in this study is clearly beyond the present technical experience. A worst-case scenario is that the formation of large bubbles results in poor gas–solids contact and large pressure fluctuations that produce technical difficulties. A consequence might be that the solids inventory needs to be reduced, which would mean lower gas conversion and solids residence time, i.e. higher loss of char to air reactor. Lower gas conversion means higher costs for oxygen production. A higher loss of char to air reactor can be addressed by the milling of fuel to finer sizes and by extending the height of the loop seal leading material from the fuel reactor to the air reactor in order to increase the residence time. A likely consequence of lowering the solids inventory in the fuel reactor is that the floor of the air reactor has to be lowered as the bed levels of the reactors are coupled via the lower loop seal.
- Difficulties with the volatiles distributor. The material cost of this device is low, so modifications should also be moderate in cost. However, this technology has not been tested and the worst-case scenario, although unlikely, is that it would be impossible to make it work. Consequently, bottom bed feeding of fuel distributed over a number of inlets would be needed to avoid excessive local concentration of the volatiles. Nevertheless, not having a volatiles distributor would lower the contact between gas and solids, which lowers gas conversion, resulting in higher costs for oxygen production. A good idea is to test the device first in a conventional boiler.
- Elutriation of char. Elutriation of char higher than expected would again increase the need for oxygen and may also lead to a loss of unburnt char if the conversion in the post-oxidation chamber is incomplete.
- Local agglomeration of bed particles. The CLC reactors operate at higher temperature than in the reference case, which could lead to risks of agglomeration depending on the sintering propensity of the fuel ash. Possible actions include change of fuel, higher exchange rate of bed material, change of oxygen carrier and lowered bed temperature. The bed temperature of the fuel reactor can be lowered by decreasing the circulation. Depending on the temperature decrease this will affect char gasification and to some extent the gas conversion. The consequence would be higher costs for oxygen production, and lowering the very high rate of $CO_2$ capture expected for this process.
- Mal-distribution over parallel cyclones. Studies of identical parallel cyclones indicate that mal-distribution over cyclones appears with gas streams of high solids loading, whereas distribution becomes stable with more dilute streams, [41]. Even with the higher loading needed for increased circulation, it is likely that the system is below the level where significant mal-distributions appear. The risk of mal-distribution can be avoided by splitting the air reactors in two by a wall. Thus there would be one air reactor for each air reactor cyclone. Such a solution could also be of interest to raise the options for part load operation.

The major risks identified involve modifications of moderate cost and/or reduced performance. There seems to be no "killers", and the only consequences would be somewhat increased costs for a technology expected to have uniquely low costs in comparison to other $CO_2$ capture technologies.

## 11. Conclusions

The design of a CLC–CFB plant is discussed with focus on the differences compared to CFB technology and what these differences mean with respect to costs. In addition to $CO_2$ compression, which is inevitable and common to all $CO_2$ capture technologies, important costs include air separation for oxy-polishing, oxygen carrier and fluidization of the fuel reactor. The cost for air separation could be low if gas conversion were high, and the cost of the oxygen carrier could be low if the life were high. The total $CO_2$ cost for capture is estimated to be 20 €/tonne $CO_2$ avoided and within the range of 16–26 €/tonne.

The cost analysis is based on tangible differences between CLC–CFB and CFB technologies, which makes the analysis transparent. Should new and better information become available the analysis can be easily updated, consequently providing a platform for further techno-economic analysis of this process.

## Acknowledgements

## References

[1] Lyngfelt A, Leckner B, Mattisson T. A fluidized-bed combustion process with inherent $CO_2$ separation; application of chemical-looping combustion. Chem Eng Sci 2001;56(10):3101–13.

[2] Lyngfelt A. Oxygen carriers for chemical-looping combustion – 4000 h of operational experience. Oil Gas Sci Technol – Revue d'IFP Energies nouvelles 2011;66(2):161–72.

[3] Adánez J, Abad A, García-Labiano F, Gayán P, de Diego L. Progress in chemical-looping combustion and reforming technologies. Progress Energy Combust Sci 2012;38(2):215–82.

[4] Lyngfelt A. Chemical-looping combustion of solid fuels – status of development. Appl Energy 2014;113:1869–73.

[5] Lyngfelt A. Chemical looping combustion. In: Scala F, editor. Fluidized-bed technologies for near-zero emission combustion and gasification. Woodhead Publishing Limited; 2013. p. 895–930.

[6] Lewis W, Gilliland E, Sweeney M. Gasification of carbon. Chemical Engineering Progress 1951;47(5):251–6.

[7] Dennis JS, Scott SA, Hayhurst AN. In situ gasification of coal using steam with chemical looping: a technique for isolating $CO_2$ from burning a solid fuel. J Energy Instit 2006;79(3):187–90.

[8] Cao Y, Casenas B, Pan WP. Investigation of chemical looping combustion by solid fuels. 2. Redox reaction kinetics and product characterization with coal, biomass, and solid waste as solid fuels and CuO as an oxygen carrier. Energy Fuels 2006;20(5):1845–54.

[9] Leion H, Mattisson T, Lyngfelt A. The use of petroleum coke as fuel in chemical-looping combustion. Fuel 2007;86(12–13):1947–58.

[10] Leion H, Mattisson T, Lyngfelt A. Solid fuels in chemical-looping combustion. Int J Greenhouse Gas Control 2008;2(2):180–93.

[11] Berguerand N, Lyngfelt A. Design and operation of a 10 $kW_{th}$ chemical-looping combustor for solid fuels – testing with South African coal. Fuel 2008;87(12):2713–26.

[12] Berguerand N, Lyngfelt A. The use of petroleum coke as fuel in a 10 $kW_{th}$ chemical-looping combustor. Int J Greenhouse Gas Control 2008;2(2):169–79.

[13] Shen L, Wu J, Xiao J. Experiments on chemical looping combustion of coal with a NiO based oxygen carrier. Combust Flame 2009;156(3):721–8.

[14] Cuadrat A, Abad A, García-Labiano F, Gayán P, de Diego LF, Adánez J. The use of ilmenite as oxygen-carrier in a 500 $W_{th}$ chemical-looping coal combustion unit. Int J Greenhouse Gas Control 2011;5(6):1630–42.

[15] Wu J, Shen L, Hao J, Gu H. Chemical looping combustion of coal in a 1 $kW_{th}$ reactor. In: 1st International conference on chemical looping. Lyon; 2010.

[16] Linderholm C, Lyngfelt A, Cuadrat A, Jerndal E. Chemical-looping combustion of solid fuels – operation in 10 kW unit with two fuels, above-bed and in-bed fuel feed and two oxygen carriers, manganese ore and ilmenite. Fuel 2012;102:808–22.

[17] Sozinho T, Pelletant W, Gauthier T, Stainton H. Main results of the 10 kW coal pilot plant operation. In: 2nd Int. conf. on chemical looping. Darmstadt; 2012.

[18] Thon A, Kramp M, Hartge EU, Heinrich S, Werther J. Operational experience with a system of coupled fluidized beds for chemical looping combustion of solid fuels using ilmenite as oxygen carrier. Appl Energy 2014;118:309–17.

[19] Tong A, Bayham S, Kathe M, Zeng L, Luo S, Fan L-S. Iron-based syngas chemical looping process and coal-direct chemical looping process development at Ohio State University. In: 2nd International conference on chemical looping. Darmstadt; 2012.

[20] Markström P, Linderholm C, Lyngfelt A. Chemical-looping combustion of solid fuels – design and operation of a 100 kW unit with bituminous coal. Int J Greenhouse Gas Control 2013;15:150–62.

[21] Linderholm C, Knutsson P, Schmitz M, Markström P, Lyngfelt A. Material balances of carbon, sulfur, nitrogen and ilmenite in a 100 kW CLC reactor system. Int J Greenhouse Gas Control 2014;27:188–202.

[22] Bayham S, Kim H, Wang D, Tong A, Zeng L, McGiveron O, et al. Iron-based coal direct chemical looping combustion process: 200-h continuous operation of a 25-$kW_{th}$ subpilot unit. Energy Fuels 2013;27:1347–56.

[23] Abdulally I, Beal C, Andrus H, Epple B, Lyngfelt A, White B. Alstom's chemical looping technology, program update. In: 11th Annual conference on carbon capture utilization & sequestration. Pittsburgh (Pennsylvania); 2014.

[24] Ströhle J, Orth M, Epple B. Chemical looping combustion of hard coal in a 1 $MW_{th}$ Pilot Plant Using Ilmenite as Oxygen Carrier, Applied Energy, 2015, submitted for publication.

[25] Pérez-Vega R, Abad A, Gayán P, de Diego LF, García-Labiano F, Adánez J. Design and operation of a 50 $kW_{th}$ chemical looping combustion (CLC) pilot plant with solid fuel, Applied Energy, 2015, submitted for publication.

[26] Lyngfelt A, Mattisson T. Oxygen carriers for chemical-looping combustion. In: Fennell P, Anthony EJ, editors. Calcium and chemical looping technology for power generation and carbon dioxide ($CO_2$) capture. Woodhead Publishing; 2014. Chapter 11.

[27] Linderholm C, Adánez J, Béal C, Epple B, Penthor S, Larring Y, Lyngfelt A. Chemical-looping coal combustion – results from the ACCLAIM project. In: 3rd International conference on chemical looping. Gothenburg; 2014.

[28] Ekström C, Schwendig F, Biede O, Franco F, de Koeijer G, et al. Techno-economic evaluations and benchmarking of pre-combustion $CO_2$ capture and oxy-fuel processes developed in the European ENCAP project. Energy Procedia 2009;1:4233–40.

[29] Rose JW, Cooper JR. Technical data on fuel, 7th edition. Edinburgh: The British National Committee, World Energy Conference; 1977.

[30] Yue G, Lu J, Zhang H, Yang H, Zhang J, Liu Q, Jaud P. Design theory of circulating fluized bed boilers. In: 18th International conference on fluidized bed combustion. Toronto (Canada); 2005.

[31] Wu H, Zhang M, Sun Y, Lu Q, Na Y. Research on the heat transfer model of platen heating surface of 300 MW circulating fluidized bed boilers. Powder Technol 2012;226:83–90.

[32] Johnsson F, Leckner B. Vertical distribution of solids in a CFB-furnace. In: 13th Int. conf. fluid. bed comb. Orlando; 1995, p. 671–9.

[33] Johansson E, Lyngfelt A, Mattisson T, Johnsson F. A circulating fluidized bed combustor system with inherent $CO_2$ separation – application of chemical looping combustion. In: 7th Int. conf. on circulating fluidized beds. Niagara Falls (Ontario); 2002.

[34] Markström P, Linderholm C, Lyngfelt A. Analytical model of gas conversion in a 100 kW chemical-looping combustor for solid fuels – comparison with operational results. Chem Eng Sci 2013;96:131–41.

[35] Abad A, Adánez J, Cuadrat A, García-Labiano F, Gayán P, de Diego LF. Kinetics of redox reactions of ilmenite for chemical-looping combustion. Chem Eng Sci 2011;66(4):689–702.

[36] Hallberg P, Leion H, Lyngfelt A. A method for determination of reaction enthalpy of oxygen carriers for chemical looping combustion – application to ilmenite. Thermochim Acta 2011;524:62–7.

[37] Lyngfelt A, Pallarés D, Linderholm C, Rydén M, Mattisson T. Fördelare av gaser i fluidiserad bädd ("Distributor of volatile gasis in the bottom part of a fluidized bed"), Swedish patent application No. 1400085-5. 2014.

[38] Kolbitsch P, Bolhàr-Nordenkampf J, Pröll T, Hofbauer H. Operating experience with chemical looping combustion in a 120 kW dual circulating fluidized bed (DCFB) unit. Int J Greenhouse Gas Control 2010;4(2):180–5.

[39] Hu N, Yang HR, Zhang H, Zhang RQ, Cao JN, Liu Q, Yue GX. Experimental study on gas-solid flow characteristics in a CFB riser of 54 m in height. In: 20th Int. Conf. on FBC. Xian (China); 2010.

[40] Basu P, Chandel M, Butler J, Dutta A. An investigation into the operation of the twin-exit loop-seal of a circulating fluidized bed boiler in a thermal power plant and its design implication. J Energy Resour Technol 2009;131(4). 041401/1-8.

[41] Masnadi M, Grace JR, Elyasi S, Bi X. Distribution of multi-phase gas–solid flow across identical parallel cyclones: modeling and experimental study. Separat Purificat Technol 2010;72(1):48–55.